Probing carrier populations in ZnO quantum wells by screening of the internal electric fields

A. Chernikov, S. Schäfer, M. Koch, and S. Chatterjee
Faculty of Physics and Materials Sciences Center, Philipps-Universität Marburg, Renthof 5, D-35032 Marburg, Germany

B. Laumer
Walter Schottky Institut, Technische Universität München, Am Coulombwall 4, D-85748 Garching

M. Eickhoff
I. Physikalisches Institut, Justus-Liebig-Universität Gießen, Heinrich-Buff-Ring 16, D-35392 Gießen, Germany
(Received 27 August 2012; revised manuscript received 16 November 2012; published 22 January 2013)

We investigate the carrier relaxation from (ZnMg)O barrier layers into a ZnO quantum well (QW) by following the dynamic screening of its built-in electric fields. The respective emission lines shift in energy as the carriers populate the QW, spectrally shifting the time-resolved photoluminescence. At low temperatures, the carrier capture into the QW is found to occur on the same or an even faster time scale than the carrier-trapping processes within the barriers.

DOI: 10.1103/PhysRevB.87.035309 PACS number(s): 78.67.De, 78.55.Cr, 78.47.jd

ZnO is a direct-gap II-VI semiconductor with the band gap in the UV spectral range adopting the hexagonal wurtzite crystal structure. The optical response of the bulk material has been widely studied over the past decades and a comprehensive review of the material properties is, e.g., given in Refs. 1–4. More recently, ZnO quantum wells (QWs) with (ZnMg)O barriers have become available due to improved growth methods.[5–11] This system is proposed for the application of ZnO in electro-optical devices such as photodetectors, light-emitting diodes, and, above all, lasers in the UV spectral range, attracting much interest in the scientific community.[12–17] All these applications have in common that, in general, their performance is highly sensitive to the carrier dynamics. Hence, acquiring this detailed knowledge remains a crucial task for the optimal design as well as the efficient operation of ZnO-based devices.

In this paper, we study the carrier relaxation from (ZnMg)O barriers into a ZnO single via time-resolved photoluminescence (PL) spectroscopy. Typically, emission spectroscopy does not always allow for an unambiguous measurement of the carrier populations, particularly in systems with translational symmetry. In general, the rise of the PL signal is determined by both carrier density and carrier temperature since radiative recombination rates are much lower in the case of hot carrier distributions.[18] Here, we develop an experimental procedure circumventing these issues. One of the hallmarks of heterostructures fabricated from materials crystallizing in the wurtzite structure is the occurrence of polarization-induced electric fields.[19–21] These fields strongly influence the optical properties of the material system, leading to, e.g., the quantum-confined Stark effect (QCSE).[22–24] The built-in electric fields cause a spatial separation of electron and hole wave functions resulting in an increase of the radiative lifetime and a shift of the transition towards lower energy. Its magnitude is rather sensitive to the carrier density in the system due to the Coulomb-mediated screening of the internal fields.[25–27] In addition, the "rearrangement" of carriers inside the QW leading to the buildup of screening is expected to occur on an ultrafast time scale of less than 1 ps.[27,28] In our experiments we exploit screening phenomena for a direct observation of the carrier population inside a QW with a built-in electric field and apply the developed technique to the ZnO/(ZnMg)O material system.

The time-resolved photoluminescence (PL) measurements are performed using a conventional streak-camera setup[29] with a tunable pulsed 100 fs excitation. The achieved time and spectral resolution are 3 ps and 0.5 nm, respectively. The (Zn,Mg)O/ZnO single quantum well investigated in this study is grown by plasma-assisted molecular beam epitaxy[5] at a low substrate temperature of 270 °C and under highly metal-rich growth conditions.[11,30] The bottom $Zn_{0.72}Mg_{0.28}O$ barrier with a thickness of 70 nm is directly deposited on the $(11\bar{2}0)$ sapphire substrate and was annealed at 560 °C for 5 min in order to improve the abruptness of the heterointerface. Subsequently, the 7 nm wide ZnO quantum well and the top $Zn_{0.72}Mg_{0.28}O$ barrier are grown without any further growth interruptions. The relatively wide quantum well width ensures that the influence of polarization-induced internal electric field becomes apparent. From the redshift of the QW PL emission peak and comparison to simulations performed with NEXTNANO^3 its magnitude is estimated to 750 kV/cm.[31] The thickness of the top barrier was also chosen to be 70 nm in order to inhibit screening of internal electric fields by surface accumulated charge carriers.

Initially, the samples are characterized by low-power PL with a photon flux of 3×10^{12} cm^{-2} per pulse at a photon energy of 4.3 eV. Thus, the incident light is mainly absorbed in the (ZnMg)O barriers. The emission is integrated over 2 ns following the excitation and the resulting PL spectrum is plotted in Fig. 1. A pronounced peak from the QW emission is observed along with several phonon-assisted transitions, i.e., phonon sidebands (PSBs), below. The corresponding PL transient at the QW energy indicated by the vertical dashed line is shown in the inset. The luminescence signal at negative times is observed due to the long carrier lifetimes and 80 MHz repetition rate of the laser. The emission peak at 3.19 eV below the bulk value of about 3.38 eV as well as the long decay time of the PL signal are both clear signatures of the QCSE present

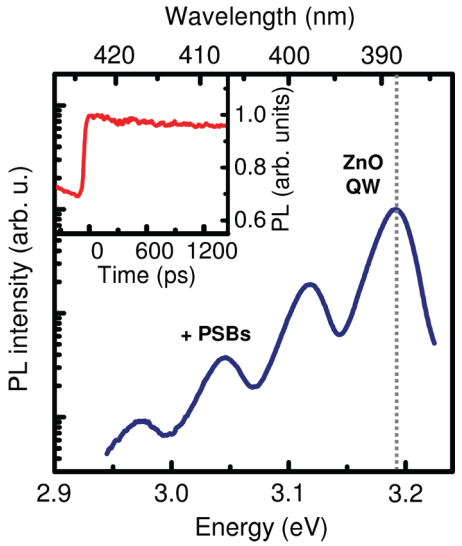

FIG. 1. (Color online) Low-temperature PL spectrum of the ZnO QW for the excitation density of 3×10^{12} cm^2 photons per pulse. The corresponding transient of the zero-phonon emission indicated by the dashed vertical line is shown in the inset.

in the QW sample. The energy of the QW PL corresponds well to the data reported for ZnO/(ZnMgO) heterostructures with similar well widths and Mg contents.[32]

Figure 2(a) shows several emission spectra from the ZnO QW for various delay times after excitation with a low excitation density of 3×10^{12} cm^{-2}. The spectra resemble the time-integrated emission plotted in Fig. 1 and the PL

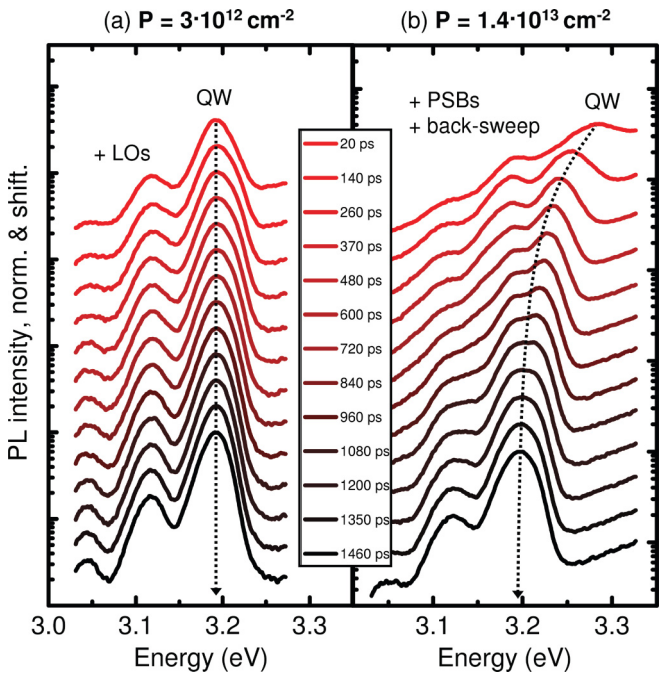

FIG. 2. (Color online) PL spectra of a ZnO/($Zn_{0.72}Mg_{0.28}$)O QW with $d = 7$ nm for two different pump densities of 3×10^{12} and 1.4×10^{13} cm^{-2} photons per pulse for various time delays after the excitation. All spectra are integrated over a time window of 120 ps. The data are normalized and shifted for clarity. The lattice temperature is set to 10 K.

maximum remains at a constant energy for all times; merely a slight excitation-induced broadening is observed shortly after the excitation. For comparison, the corresponding data at a higher pump-power density 1.4×10^{13} cm^{-2} photons per pulse are shown in Fig. 2(b). Again, all spectra exhibit pronounced QW PL with the low-energy flank dominated by the phonon-assisted emission peaks. However, for the high-power conditions, the PL exhibit an initial shift to higher energies of about 90 meV, in stark contrast to the low density case shown in Fig. 2(a). At longer times the emission maximum shifts back towards lower energies; additionally, some contributions from the so-called "back-sweep" artefact in the streak camera appear in the spectra. The pronounced energy shift observed at high pump densities is characteristic for the Coulomb-mediated screening.[32,33] The carriers within the QW screen the internal field, thus weakening the QCSE. This leads to faster radiative recombination due to an increased overlap of the electron and hole wave functions as well as to a pronounced shift of the respective energy levels of electrons and holes towards higher energies. As the carriers recombine, the effect of screening also decreases, following the decrease of the carrier density. Hence, at longer time delays after the excitation, the emission maximum returns to the initial, unscreened position in energy corresponding to the low-power excitation conditions.

The influence of carrier density-dependent screening on the emission properties of the QW is summarized in Fig. 3. The PL energy maximum [Fig. 3(a)], the effective $1/e$ decay time [Fig. 3(b)], and the integrated intensity [Fig. 3(c)] are

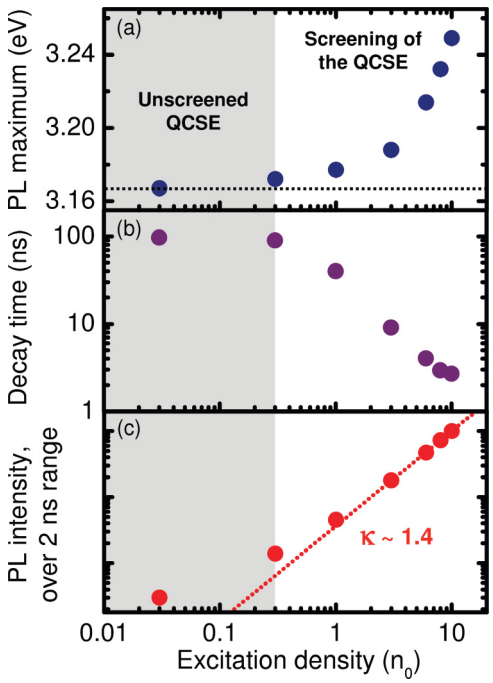

FIG. 3. (Color online) (a) PL energy maximum, (b) effective $1/e$ decay time, and (c) the integrated intensity of the ZnO/($Zn_{0.72}Mg_{0.28}$)O QW with $d = 7$ nm as a function of the excitation density for a lattice temperature of 10 K. The excitation density is normalized to the photon flux of $n_0 = 10^{12}$ cm^{-2} per pulse. κ denotes the exponent extracted from the dependence of the PL intensity I_{PL} on the pump power, $I_{PL} = I_{pump}^{\kappa}$.

plotted as a function of the excitation power density, which is a measure of the carrier density directly after the excitation pulse. The effective decay time is defined as an average $1/e$ decay from the PL maximum with the respect to the residual PL background. The latter appears due to the 80 MHz repetition rate of the laser as well as a slow decay of the luminescence signal on the ns time scale. The emission maximum is extracted from the PL spectra, integrated over a window directly after the excitation from 0 to 50 ps. As the pump-power density increases, the maximum of the PL emission strongly shifts towards higher energies. This behavior is accompanied by a decrease of the decay time by about two orders of magnitude. At the same time, a strong, superlinear increase of the emitted intensity with increasing pump power is observed, quantified by fitting a power function with an exponent of 1.4. Thus, we attribute the decrease of the carrier lifetime to a faster radiative recombination that is also manifested in the increased decay rate. Hence, an alternative interpretation of the experimental findings as saturation of the localized states is clearly excluded. In the latter case, the PL intensity dependence on the excitation density would show a linear trend at best or even a sublinear behavior.[34] According to the PL data, the density-dependent screening of the QCSE is a strongly nonlinear process allowing to subdivide the excitation regimes in regions of an unscreened and screened QCSE. Here, it should be noted that since the PL maximum is always below the energy of the ZnO bulk transition, corresponding to a fully screened electric field, the term "screened QCSE" should be understood as a substitute for "*partially* screened QCSE."

In addition, the features in the optical response of the investigated ZnO/(ZnMg)O heterostructure related to the screening of the internal field are comparable to the well-studied GaN-based systems. Typically, the properties of the GaN/(AlGa)N and (InGa)N/GaN quantum wells are also strongly influenced by the QCSE, leading to a redshift of the electron-hole states as well as to a slow radiative decay in the 10 ns range.[35,36] After an optical injection of charge carriers by a short laser pulse, the overall dynamics of the following QW emission exhibit both a transient blueshift as well as a faster decay.[36–38] The recombination times also change over orders of magnitude with increased carrier density.[36,37] A detailed quantitative comparison of the energy shifts and recombination dynamics in the GaN- and ZnO-based systems would further require elaborate theoretical calculations taking into account specific sample properties such as nonradiative recombination or disorder.

Finally, we extract the carrier densities from the screening dynamics. Based on the results shown in Fig. 3, the excitation density of $6n_0$ is chosen for the study of the buildup of screening charge. Therefore, the temporal detection window is set to 50 ps instead of 2 ns, corresponding to the effective time resolution of less than 3 ps. In addition, the streak camera is operated with an active synchronous blanking unit to avoid any contributions from the "back sweep." Transient PL spectra are extracted by integrating over a 2 ps interval, shown in Fig. 4(a) as a function of the time delay after the excitation. The corresponding streak-camera image with the PL intensity plotted as a function of the emission energy and time is shown in Fig. 4(b). Again, the PL signal at negative times results from the remaining carrier population in the

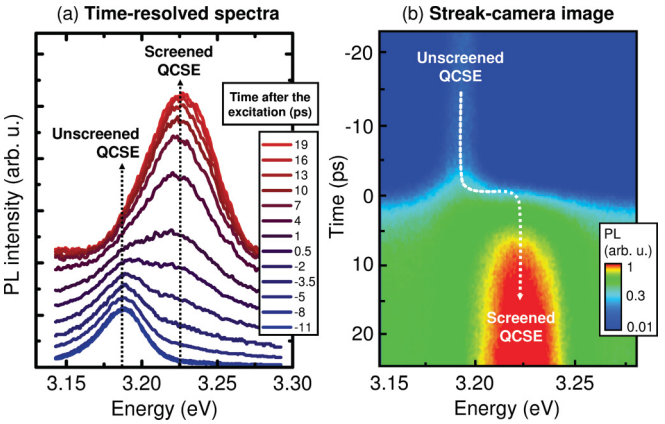

FIG. 4. (Color online) (a) Transient PL spectra of the ZnO/($Zn_{0.72}Mg_{0.28}$)O QW with $d = 7$ nm for an excitation density of $6n_0$ per pulse and a lattice temperature of 10 K. (b) Corresponding image of the streak camera with the PL intensity plotted as a function of emission energy and time delay after the excitation.

QW, created by the previous laser pulse incident 12.5 ns earlier onto the sample. At $t = 0$ ps, as the excitation pulse arrives, the emission peak attributed to the screened QCSE appears almost instantaneously at the high-energy flank of the "unscreened" PL. At later delay times, the intensity of the "screened" luminescence increases, yet the energy of the peak does not exhibit any additional shift. The overlap between the two peaks is due to the convolution of the signals with a Gaussian with a full width at half maximum (FWHM) of 3 ps, corresponding to the time resolution of the setup. Hence, the buildup of the "screened" PL is virtually instantaneous within the experimental uncertainty. In general, the corresponding time scale is determined by the faster of the two following processes: the rise of the carrier population and the buildup of screening. It should be noted, however, that the time scale for the latter is in the range of 100 fs, corresponding to the length of the excitation pulse (see, e.g., Ref. 28). The time constant is roughly estimated from the inverse plasma frequency in the excited electron-hole system,[23] using ZnO material parameters[39] and approximate carrier densities for the applied excitation conditions.

Figure 5 summarizes the dependence of the PL maximum as well as the integrated PL intensity on the delay time after the excitation. In addition, the corresponding carrier densities are shown, extracted from the PL energies using the data from Fig. 3(a). The QW carrier population increases almost instantaneously at $t = 0$ ps, i.e., within the experimental resolution of 3 ps, in strong contrast to the slowly rising luminescence intensity. The increase of the PL on the time scale of several tens of ps is thus clearly attributed to carrier relaxation, i.e., cooling processes, inside the QW. Hence, as a main result, the capture of carriers, excited in the (ZnMg)O barriers, into the QW occurs within the first 3 ps.

It should be also mentioned that we still observe a residual PL from the (ZnMg)O barriers. The intensity of the emission is comparable to the QW luminescence, which is typical for ZnO/(ZnMg)O heterostructures.[10,30] However, for the chosen excitation conditions nearly all carriers are created inside the (ZnMg)O layers due to a rather large corresponding width of

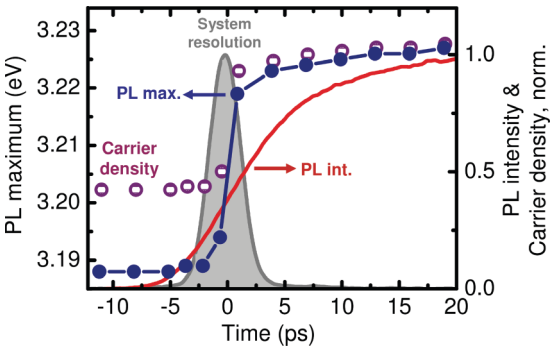

FIG. 5. (Color online) PL maximum, resulting carrier population, as well as the integrated emission intensity of the ZnO/$(Zn_{0.72}Mg_{0.28})$O QW with $d = 7$ nm as a function of time delay after the excitation. The excitation density is set to $6n_0$ and the lattice temperature is 10 K. The system resolution is shown by the gray area for comparison.

70 nm and an initially weak coupling of the QW to the light field. Thus, about a half of the photoexcited carriers are captured in the QW. Also, no additional feeding of the QW population is observed on a time scale corresponding to the decay time of the (ZnMg)O PL in the order of several hundreds of ps. Therefore, the residual emission from the barrier layers is attributed to strongly localized carriers due to potential fluctuations and disorder in (ZnMg)O alloy structures.[29]

In summary, the concept of monitoring the QW carrier population by exploiting screening phenomena is introduced and verified. As a result, the capture of carriers from the (ZnMg)O barriers into the ZnO QW is found to occur on an ultrafast time scale below 3 ps, limited by the experimental resolution. This fast relaxation is observed despite a rather high Mg concentration in the (ZnMg)O layers, which leads to pronounced potential fluctuations and carrier localization (see Ref. 29). Hence, the carrier capture into the QW occurs on the same or an even faster time scale than the carrier-trapping processes within the barriers. Such a behavior should be a significant benefit for the operation of optical devices based on ZnO-heterostructures.

The authors would like to thank Stephan W. Koch for fruitful and constructive discussions.

[1]U. Özgür, Y. I. Alivov, C. Liu, A. Teke, M. A. Reshchikov, S. Dogan, V. Avrutin, S.-J. Cho, and H. Morkoc, J. Appl. Phys. **98**, 041301 (2005).
[2]C. F. Klingshirn, B. K. Meyer, A. Waag, A. Hoffmann, and J. Geurts, *Zinc Oxide*, Springer Series in Materials Science, Vol. 120 (Springer, Berlin, 2010).
[3]C. Klingshirn, J. Fallert, H. Zhou, J. Sartor, C. Thiele, F. Maier-Flaig, D. Schneider, and H. Kalt, Phys. Status Solidi B **247**, 1424 (2010).
[4]L. Brillson and Y. Lu, J. Appl. Phys. **109**, 121301 (2011).
[5]A. K. Sharma, J. Narayan, J. F. Muth, C. W. Teng, C. Jin, A. Kvit, R. M. Kolbas, and O. W. Holland, Appl. Phys. Lett. **75**, 3327 (1999).
[6]T. Makino, C. H. Chia, N. T. Tuan, H. D. Sun, Y. Segawa, M. Kawasaki, A. Ohtomo, K. Tamura, and H. Koinuma, Appl. Phys. Lett. **77**, 975 (2000).
[7]W. I. Park, G.-C. Yi, and H. M. Jang, Appl. Phys. Lett. **79**, 2022 (2001).
[8]S. Muthukumar, J. Zhong, Y. Chen, Y. Lu, and T. Siegrist, Appl. Phys. Lett. **82**, 742 (2003).
[9]S. Sadofev, S. Blumstengel, J. Cui, J. Puls, S. Rogaschewski, P. Schafer, Y. G. Sadofyev, and F. Henneberger, Appl. Phys. Lett. **87**, 091903 (2005).
[10]J.-M. Chauveau, M. Laügt, P. Venneguès, M. Teisseire, B. Lo, C. Deparis, C. Morhain, and B. Vinter, Semicond. Sci. Technol. **23**, 035005 (2008).
[11]T. A. Wassner, B. Laumer, S. Maier, A. Laufer, B. K. Meyer, M. Stutzmann, and M. Eickhoff, J. Appl. Phys. **105**, 023505 (2009).
[12]A. Bakin, A. El-Shaer, A. C. Mofor, M. Al-Suleiman, E. Schlenker, and A. Waag, Phys. Status Solidi C **4**, 158 (2007).
[13]T. V. Shubina, A. A. Toropov, O. G. Lublinskaya, P. S. Kopev, S. V. Ivanov, A. El-Shaer, M. Al-Suleiman, A. Bakin, A. Waag, A. Voinilovich, E. V. Lutsenko, G. P. Yablonskii, J. P. Bergman, G. Pozina, and B. Monemar, Appl. Phys. Lett. **91**, 201104 (2007).
[14]J. W. Sun and B. P. Zhang, Nanotechnology **19**, 485401 (2008).
[15]S.-M. Li, B.-J. Kwon, H.-S. Kwack, L.-H. Jin, Y.-H. Cho, Y.-S. Park, M.-S. Han, and Y.-S. Park, J. Appl. Phys. **107**, 033513 (2010).
[16]J. Zippel, M. Stölzel, A. Müller, G. Benndorf, M. Lorenz, H. Hochmuth, and M. Grundmann, Phys. Status Solidi B **247**, 398 (2010).
[17]G. Tabares, A. Hierro, B. Vinter, and J.-M. Chauveau, Appl. Phys. Lett. **99**, 071108 (2011).
[18]L. Andreani, Solid State Commun. **77**, 641 (1991).
[19]F. Bernardini, V. Fiorentini, and D. Vanderbilt, Phys. Rev. B **56**, R10024 (1997).
[20]S.-H. Park and S.-L. Chuang, J. Appl. Phys. **87**, 353 (2000).
[21]C. Morhain, T. Bretagnon, P. Lefebvre, X. Tang, P. Valvin, T. Guillet, B. Gil, T. Taliercio, M. Teisseire-Doninelli, B. Vinter, and C. Deparis, Phys. Rev. B **72**, 241305 (2005).
[22]D. A. B. Miller, D. S. Chemla, T. C. Damen, A. C. Gossard, W. Wiegmann, T. H. Wood, and C. A. Burrus, Phys. Rev. B **32**, 1043 (1985).
[23]C. Klingshirn, *Semiconductor Optics*, 2nd ed. (Springer, Berlin, 2007).
[24]M. Lange, J. Kupper, C. P. Dietrich, M. Brandt, M. Stölzel, G. Benndorf, M. Lorenz, and M. Grundmann, Phys. Rev. B **86**, 045318 (2012).
[25]H. Haug and S. W. Koch, *Quantum Theory of the Optical and Electronic Properties of Semiconductors*, 5th ed. (World Scientific, Singapore, 2009).
[26]D. Turchinovich, B. S. Monozon, and P. U. Jepsen, J. Appl. Phys. **99**, 013510 (2006).
[27]C. R. Hall, L. Dao, K. Koike, S. Sasa, H. H. Tan, M. Inoue, M. Yano, P. Hannaford, C. Jagadish, and J. A. Davis, Phys. Rev. B **80**, 235316 (2009).
[28]R. Huber, F. Tauser, A. Brodschelm, M. Bichler, G. Abstreiter, and A. Leitenstorfer, Nature (London) **414**, 286 (2001).

[29] A. Chernikov, S. Horst, M. Koch, K. Volz, S. Chatterjee, S. Koch, T. Wassner, B. Laumer, and M. Eickhoff, J. Lumin. **130**, 2256 (2010).

[30] B. Laumer, T. A. Wassner, F. Schuster, M. Stutzmann, J. Schörmann, M. Rohnke, A. Chernikov, V. Bornwasser, M. Koch, S. Chatterjee, and M. Eickhoff, J. Appl. Phys. **110**, 093513 (2011).

[31] B. Laumer, F. Schuster, T. A. Wassner, M. Stutzmann, M. Rohnke, J. Schormann, and M. Eickhoff, J. Appl. Phys. **111**, 113504 (2012).

[32] T. Makino, Y. Segawa, A. Tsukazaki, A. Ohtomo, and M. Kawasaki, Appl. Phys. Lett. **93**, 121907 (2008).

[33] D. Turchinovich, P. U. Jepsen, B. S. Monozon, M. Koch, S. Lahmann, U. Rossow, and A. Hangleiter, Phys. Rev. B **68**, 241307 (2003).

[34] M. Urban, H. Schwab, and C. Klingshirn, Phys. Status Solidi B **166**, 423 (1991).

[35] J. C. Harris, T. Someya, S. Kako, K. Hoshino, and Y. Arakawa, Appl. Phys. Lett. **77**, 1005 (2000).

[36] T. Kuroda, A. Tackeuchi, and T. Sota, Appl. Phys. Lett. **76**, 3753 (2000).

[37] P. Lefebvre, S. Kalliakos, T. Bretagnon, P. Valvin, T. Taliercio, B. Gil, N. Grandjean, and J. Massies, Appl. Phys. Lett. **76**, 3753 (2000).

[38] Y. S. Park, H. Im, and T. W. Kang, Appl. Phys. Lett. **90**, 161922 (2007).

[39] *Semiconductors*, edited by K.-H. Hellwege, O. Madelung, M. Schulz, and H. Weiss, Landolt-Börnstein, New Series, Group III, Vol. 17, Pt. B (Springer, Berlin, 1982).